Turbulence intensity pulse propagation with self-consistent nonlinear noise

Z. H. Wang,[1,2] P. H. Diamond,[2,3] Ö. D. Gürcan,[4] X. Garbet,[5] and X. G. Wang[6]
[1]*School of Physics and Optoelectronic Technology, Dalian University of Technology, Dalian 116024, China*
[2]*Department of Physics and Center for Astrophysics and Space Sciences, University of California at San Diego, La Jolla, California 92093-0424, USA*
[3]*WCI Center for Fusion Theory, National Fusion Research Institute, Gwahangno 113, Yuseong-gu, Daejeon 305-333, South Korea*
[4]*Laboratoire de Physique des Plasmas, Ecole Polytechnique–CNRS, 91128 Palaiseau Cedex, France*
[5]*CEA, IRFM, F-13108 Saint Paul Lez Durance, France*
[6]*School of Physics, Peking University, Beijing 100871, China*

(Received 2 January 2011; accepted 17 February 2011; published online 22 March 2011)

A model of turbulence intensity spreading with self-consistent nonlinear noise is derived systematically for the simple dynamical model of resistivity gradient driven turbulence. Local effective drive, thermal conduction damping, nonlinear coupling, and spatial scattering effects are included. As a consequence of nonlinear mode coupling processes (i.e., triad mode interactions), turbulence energy can be spatially scattered, leading to turbulence propagation and spreading. However, the range of any nonlinear mode interactions of the background with a test mode is restricted to within a few mode scale widths from the test mode rational surface. The speed of a turbulent spreading front is calculated. This front speed is effectively constant on macroscopic scales. We show that the effect of self-consistent nonlinear noise on the intensity front speed is modest, as a consequence of the ordering $\Delta_c < L_f$, where Δ_c is the turbulence correlation length and L_f is the scale length of the front's leading edge. The implications of these results for turbulence spreading models and the important differences between self-consistent mode coupling noise and *ad hoc* external noise are discussed. The broader implications of these results for turbulence front propagation are identified and explained. © *2011 American Institute of Physics*.
[doi:10.1063/1.3567142]

I. INTRODUCTION

In tokamak plasmas, transport can be induced by local instabilities leading to a mixing process. The typical diffusivity is thought to obey gyro-Bohm (GB) scaling, $D_{\mathrm{GB}} \sim \rho_s^2 c_s / a$, with the mixing or correlation scale length of $\Delta_c \sim \rho_s$, where ρ_s is the ion gyroradius, c_s is the ion sonic speed, and a is the tokamak minor radius. However, breaking of GB scaling has been observed, e.g., especially by fast transients, observed in "cold pulse" experiments.[1–3] The characteristic time scale of such transient responses is about two orders of magnitude smaller than that of the typical heat diffusion time a^2/D_{GB} predicted. Such mismatches suggest that the true turbulence dynamics is more subtle than simple diffusion. Also, inward ballistic (or superdiffusive) fronts of a cold pulse are also observed in fast transient experiments.[4,5] Explaining the fast time scale of the transient response is a major challenge.

To understand the breaking of average GB scaling, simulations of both turbulence spreading[6,7] and avalanches have been done to study turbulence front dynamics on mesoscales l_{meso}. Mesoscales are larger than the mode or eddy correlation length but smaller than the system or mean profile length scale $\rho_s < l_{\mathrm{meso}} < a$. Turbulence spreading[8–15] propagates or delocalizes the free energy from the unstable to stable region mainly via nonlinear (NL) coupling interactions, which scatter turbulence intensity, and therefore facilitates transport of fluctuation energy in space. The avalanche depends strongly on the critical gradient (CG) of the mean profile, can be related to self-organized criticality[16–21] phenomena, and may be thought of as sequential overturning or toppling of the local gradient in response to a local exceedance of the threshold. Thus, both turbulence spreading and avalanche are possible mechanisms to explain the breaking of GB scaling.[22] Nevertheless, while the avalanche is primarily a process of profile evolution, it also induces turbulence spreading. It is thus ultimately hard to decouple "spreading" and "avalanche" in a system where the gradient evolves self-consistently. In this paper, though, we focus on turbulence spreading only for the sake of simplicity and tractability. Thus, the gradient scale length L_T is hereafter held fixed. We argue that the characteristic time scale for turbulence spreading should necessarily be roughly comparable to the characteristic avalanche propagation time.

A theoretical understanding of cold pulse induced fast transient and breaking of GB scaling has remained elusive. Thus, we turn to the theoretical framework for describing turbulence spreading in order to uncover and understand possible fast time scales. Indeed, recent advances in the developing theory of turbulence spreading have been motivated by the challenge of qualitatively modeling such pulse propagation phenomena.[8,14,23] Most recent theoretical results[24] suggest that turbulent spatial scattering growth (with a critical gradient threshold for growth) and self-consistent transport evolution are all required to model the pulse propagation. The former captures nonlinear intensity spreading through nonlinear coupling, while the latter accounts for the drive, as well as at least partially represents avalanche phenomena. To

TABLE I. Comparison of several theoretical models, with no nonlinear source terms.

Model	Equation	Effect included	Effect ignored
K-ε	Fluctuation energy K	Linear growth	Noise spectral transfer
	Dissipation ε	NL damp/diffusion	
Fokker–Planck	Fluctuation energy	Convection	Noise spectral transfer
		NL diffusion	
Critical gradient	Fluctuation energy	Linear growth	NL damping
	Mean field	NL diffusion	Noise

extend the theory, in this paper we study turbulence spreading by using turbulence intensity evolution equation including self-consistent nonlinear noise. The intensity field evolution is then formulated at the envelope field level by averaging over θ and ϕ.

To motivate the discussion, we first briefly review previous models. For example, there are three kinds of classical nonlinear models, K-ε,[25,26] Fokker–Planck (F–P),[27] and CG models,[23,24,28,29] which are compared in Table I. They all, at some level, describe the dynamics of turbulence propagation via both linear and nonlinear mechanisms. The K-ε model developed for high R_e fluid turbulence couples a fluctuation energy equation with a local dissipation equation, including linear growth term, as well as nonlinear diffusion and dissipation terms. The CG model has similar terms as the K-ε model, with an additional critical gradient effect in the growth term. The fluctuation energy evolution equation of the F–P model includes nonlinear dissipation and diffusion terms. The nonlinear noise[30] or incoherent source term is neglected in all the models. However, nonlinear dissipation and noise emission should participate together in the processes of nonlinear transfer, cascading, etc. To self-consistently conserve energy in nonlinear processes such as three mode interactions, both nonlinear emission and dissipation of fluctuation intensity are necessarily taken into account. Thus, it is natural and consistent also to investigate the effect of nonlinear noise emission on turbulence spreading. The key point is that not only can turbulence energy be spatially scattered by nonlinear diffusion, but it can also be emitted at one point and absorbed (dissipated) at a neighboring point via nonlinear mode coupling. Thus, such a spatial scattering process transfers turbulence energy in space. The question is, then, how the noise impacts intensity front propagation. As shown in Fig. 1, although nonlinear noise coexists with turbulence almost everywhere, the spatial scale of transfer is too limited to a few correlation lengths. Thus, only those modes localized to within a few correlation lengths of the front leading edge can influence the front speed. As a consequence, the inclusion of nonlinear noise induces only a modest acceleration of the turbulence intensity front.

We utilize here a simple model of resistivity gradient driven turbulence[31,32] (RGDT) to derive a thermal fluctuation intensity evolution equation for inhomogeneous turbulence. The dynamics of nonlinear mode coupling are determined by three mode interactions. These nonlinear interactions are restricted to within a range of correlation scales of the rational surface of the test mode. The correlation length of Δ_c is determined by the local balance between source and sink. Δ_c tells how far away free energy is scattered from the point where it is tapped. Thus, Δ_c is necessarily less than the scale length of the front's leading edge, i.e., $\Delta_c/L_f<1$. The emission of nonlinear noise thus occurs in a scale range wider than the mode width but narrower than the front's leading edge scale. Our calculation then shows that envelope theory with spatial scattering, local growth, and nonlinear source dissipation is adequate to describe turbulence spreading. The front of turbulence spreading will have a characteristic velocity $v_f\sim(D_T/\tau_c)^{1/2}$, where D_T is the turbulent diffusivity and τ_c is the turbulence correlation time. In a reaction-diffusion equation, the diffusive scattering D and the growth (i.e., reaction) drive γ similarly produce a constant front propagating speed $v_f\sim(\gamma D)^{1/2}$ in a quasisaturated state. This is called the Fisher front speed.[33–35] Here, we apply reaction-diffusion front theory to turbulence intensity front propagation.

The remainder of this paper is organized as follows. In Sec. II, the basic model is presented, the structure of nonlinear interaction is discussed, and a turbulence spreading model including nonlinear noise is derived. In Sec. III, we analyze the dynamics of saturation, address issues such as energy conservation, and identify the scales of the correlation length and the structure of nonlinear diffusion. In Sec. IV, the residual, i.e., the *local* nonzero difference of nonlinear noise and dissipation effects, is calculated for the test mode k. The influence of the noise on the local front speed is

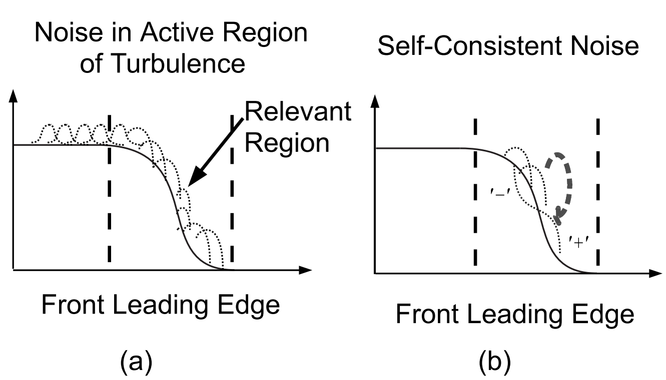

FIG. 1. (a) Nonlinear interactions relevant to influence the front speed limited to within a correlation length of the front leading edge; (b) noise as a self-consistent part of the nonlinear mode coupling process, but with a self-consistently limited range. Ultimately, $\Delta_c<L_f$ then limits the effect of self-consistent nonlinear noise.

also calculated. Section V contains discussions and conclusions. In particular, there we discuss the more general lessons learned about fast transient in the course of this work.

II. BASIC MODEL AND TURBULENCE INTENSITY EQUATION

We first derive the fluctuation intensity evolution equation for the RGDT model. This model couples the thermal fluctuation equation,

$$\frac{\partial \tilde{T}}{\partial t} + \nabla \cdot (\tilde{V}\tilde{T}) + \nabla \cdot (\tilde{V}\langle T\rangle) - \chi_{\parallel}\nabla_{\parallel}^{2}\tilde{T} = 0, \tag{1}$$

to the Ohm's law equation

$$-\nabla_{\parallel}\tilde{\phi} = \tilde{\eta}J_{z0} = \frac{c_t E_0}{\langle T\rangle}\tilde{T}. \tag{2}$$

Here, the current perturbation $\tilde{J}_z$ is assumed negligible in the region of interest, where it decouples from the potential perturbation $\tilde{\phi}$ in a "strong" electrostatic approximation. The parallel direction is approximately the toroidal or z direction. The subscript "0" indicates an average quantity, and $c_t = |d \ln \eta_0 / d \ln\langle T\rangle|$ is a proportionality coefficient, relating resistivity to temperature. The electric drift velocity,

$$\tilde{V} = \frac{\hat{z}\times\nabla\tilde{\phi}}{B_z}, \tag{3}$$

is incompressible, with $\nabla\cdot\tilde{V}=0$. Multiplying Eq. (1) by $\tilde{T}^{*}$ and then averaging over flux surface by $(4\pi^2)^{-1}\int_0^{2\pi}d\theta\int dz(\cdots)$, we get the fluctuation intensity equation

$$\frac{\partial\langle\tilde{T}^2\rangle}{\partial t} + \nabla\cdot\langle\tilde{V}\tilde{T}^2\rangle + 2(\langle\tilde{V}\tilde{T}^{*}\rangle\cdot\nabla\langle T\rangle - \chi_{\parallel}\nabla_{\parallel}^{2}\langle\tilde{T}^2\rangle) = 0. \tag{4}$$

Here, the thermal fluctuation is

$$\tilde{T}(r,\theta,z,t) = \sum_{k_\theta,k_z}\tilde{T}_k(r-r_k,t)\exp(ik_\theta r\theta + ik_z z),$$

with $\tilde{T}_k(r-r_k,t)$ being the thermal fluctuation amplitude of the mode k, depending on radial position and time. The third term on the left-hand side (LHS) of Eq. (4) then becomes an effective growth term, i.e.,

$$2\sum_k \gamma_k^{\mathrm{eff}}\langle\tilde{T}_k^2\rangle = 2\sum_k \frac{k_\theta}{k_z}\frac{c_t E_0}{B_z}\nabla\ \ln\langle T\rangle\langle\tilde{T}_k^2\rangle, \tag{5}$$

where γ_k^{eff} is the linear growth coefficient of the mode k. For a mode to grow, γ_k^{eff} has to be positive, i.e., $\gamma_k^{\mathrm{eff}}>0$. Since $(c_t E_0/B_z)\nabla\ \ln\langle T\rangle<0$, to keep γ_k^{eff} positive, k_θ and k_z are asymmetric, i.e., $k_\theta/k_z<0$. The second term on LHS of Eq. (4), involving mode-mode interactions, can be rewritten as

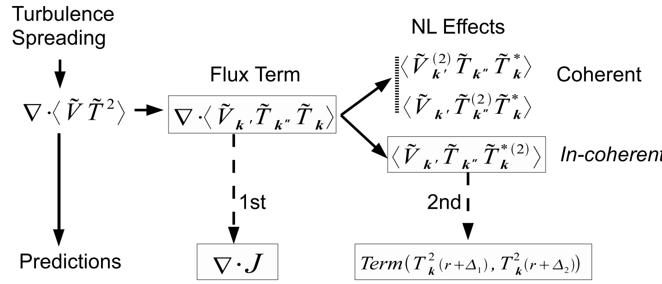

FIG. 2. Nonlinear mode coupling forms and relations.

$$\begin{aligned}\nabla\cdot\langle\tilde{V}\tilde{T}^2\rangle &= \Re\sum_k\sum_{k=k'+k''}\nabla\cdot\langle\tilde{V}_{k'}\tilde{T}_{k''}\tilde{T}_k^{*}\rangle\\ &= \Re\sum_k\sum_{k=k'+k''}\nabla\cdot(\langle\tilde{V}_{k'}\tilde{T}_{k''}\tilde{T}_k^{(2)*}\rangle + \langle\tilde{V}_{k'}\tilde{T}_{k''}^{(2)}\tilde{T}_k^{*}\rangle\\ &\quad + \langle\tilde{V}_{k'}^{(2)}\tilde{T}_{k''}\tilde{T}_k^{*}\rangle).\end{aligned} \tag{6}$$

The first term on the right-hand side (RHS) of Eq. (6) is the incoherent part of the nonlinear mode coupling, i.e., nonlinear noise, while the other two terms are the coherent parts. Thus, it is clear to make a closure based on Eq. (6) that all nonlinear interactions can be written in the form of $\nabla\cdot J$, where J is fluctuation intensity current (Fig. 2). Because fluctuations are assumed localized and radially similar to each other, we can further state that the nonlinear noise can be written as a product of $\langle\tilde{T}_k^2(r+\Delta_1)\rangle$ and $\langle\tilde{T}_k^2(r+\Delta_2)\rangle$, where Δ_1 and Δ_2 are the radial displacements from the resonant structure of mode k to that of modes k' and k'', respectively (Fig. 3). These observations are helpful to simplify and understand the structure of the triad mode interactions. The effective intensity current,

$$J_{\mathrm{eff}}(\langle\tilde{T}^2\rangle) = -D\cdot(\langle\tilde{T}^2\rangle)\nabla\langle\tilde{T}^2\rangle + V\langle\tilde{T}^2\rangle,$$

has, in principle, both nonlinear diffusion and convection parts. As we are concerned with radial propagation of a poloidal symmetric envelope, the convection velocity goes to

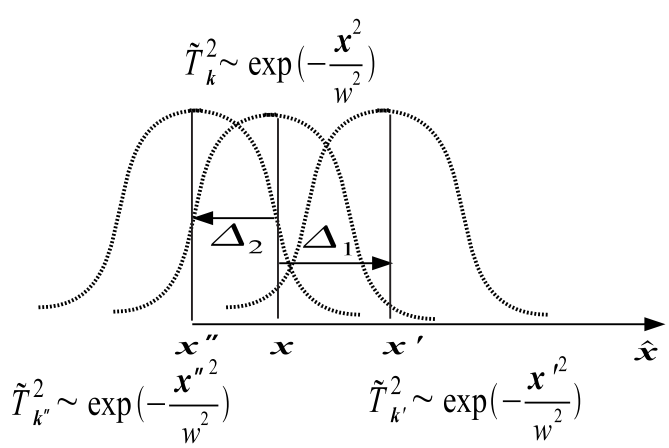

FIG. 3. Mode shifts. Δ_1 is the displacement from the test mode to background mode k', while Δ_2 is the displacement to the mode k''. All modes have the radial Gaussian structure.

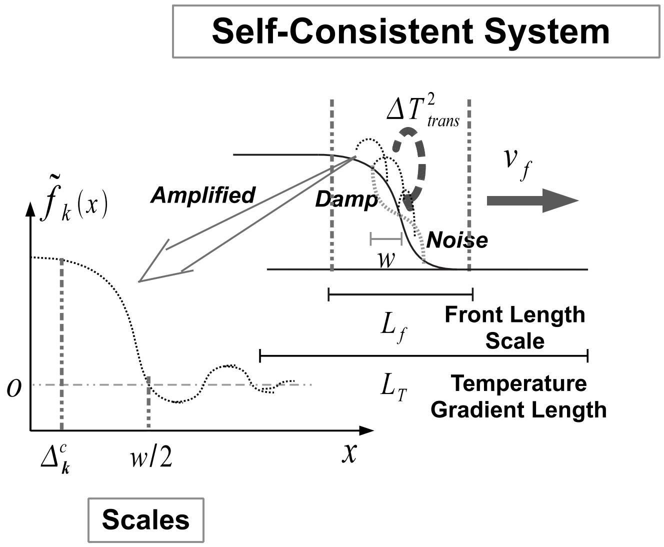

FIG. 4. Characteristic length scales.

zero, i.e., $V \rightarrow 0$. This may change for the case of an inhomogeneous magnetic field.

Before we move onto the next step, it is important to know first the characteristic length and time scales of nonlinear mode couplings. The characteristic length scales are the mode width w, correlation length Δ^c_k of the temperature fluctuation for mode k, the front scale length L_f, and the mean temperature gradient length $L_T = |d \ln\langle T\rangle/dr|^{-1}$, as shown in Fig. 4. The thermal fluctuation correlation length is roughly comparable to or less than the mode width, while the mode width is less than the front scale length, which is less than the mean temperature gradient length, i.e., $\Delta^c_k \leq w < L_f < L_T$. For localized modes, the three mode interactions are restricted to within a range of a few mode widths in space. Thermal conduction is then balanced with local effective growth and nonlinear dissipation, defining the correlation length scale. The temperature gradient length is of the system size. Thus, the scale of nonlinear mode coupling is clearly separated from the mean profile length. The characteristic time scales here are the triad mode coherence time (or wave decorrelation time) τ_c and the transient time of the front propagating through the leading edge region, L_f/v_f, i.e., L_f is the width of front leading edge and v_f is the front speed for locally saturated turbulence. For a smooth front leading edge ($\Delta^c_k < L_f$), the time scale of intensity front that propagates through the leading edge is longer than the eddy cascade time but less than the global transport time scales, i.e., $1/\tau_c > v_f/L_f > D_T/L_T^2$. For drift wave turbulence, generically, $1/\tau_c$ is set by the diamagnetic frequency, so $1/\tau_c \sim c_s/L_T$ [i.e., $k\rho_s \sim o(1)$]. Similarly, $D_T \sim D_B \rho_*^{\alpha}$, where $D_B = \rho_s c_s$ is the Bohm diffusivity, and $\rho_* = \rho_s/L_T$. Here, usually $0 < \alpha < 1$, where $\alpha = 0$ corresponds to Bohm scaling and where $\alpha = 1$ corresponds to gyro-Bohm. Thus, the intensity front speed is predicted to scale as $v_f \sim c_s \rho_*^{(1+\alpha)/2}$. Then $v_f/L_f \sim c_s \rho_*^{(1+\alpha)/2}/L_f$ is greater than $D_T/L_T^2 \sim \rho_s c_s \rho_*^{\alpha}/L_T^2 \sim c_s \rho_*^{\alpha+1}/L_T$, but less than $1/\tau_c \sim c_s/L_T$. The interesting dynamics are all on mesoscales.

Now we can calculate the second order thermal fluctuation for the mode k by expanding Eq. (1) and taking the radial velocity component only, i.e.,

$$\frac{\partial \tilde{T}_k^{(2)}}{\partial t} + (\chi_\parallel k_\parallel^2 - \gamma_k^{\mathrm{eff}})\tilde{T}_k^{(2)} = - \sum_{k=k'+k''} \tilde{V}_{rk'} \frac{\partial \tilde{T}_{k''}}{\partial r}. \tag{7}$$

The RHS of Eq. (7) can then be rewritten as[36]

$$- \sum_{k=k'+k''} \tilde{V}_{rk'} \frac{\partial \tilde{T}_{k''}}{\partial r} = - \left(\tilde{V}_{rk'} \frac{\partial \tilde{T}_{k''}}{\partial r} + \tilde{V}_{rk''} \frac{\partial \tilde{T}_{k'}}{\partial r} \right) - \gamma_k^{nl} \tilde{T}_k^{(2)}. \tag{8}$$

The terms in the parentheses are the contributions of two beat modes (k', k''), and the rest is due to the contribution of background modes. γ_k^{nl} represents the eddy-damping rate due to the interactions of test mode k with other background modes. Because the modes k' and k'' form a triad with the test mode k, the two terms in the parentheses of Eq. (8) give the same contribution. Thus, the solution of Eq. (7) is

$$\tilde{T}_k^{(2)*}(t) = -2 \int dt' \tilde{V}^*_{rk'}(t') \frac{\partial \tilde{T}^*_{k''}}{\partial r}(t') \times \exp[-(\gamma_k^{nl} - \gamma_k^{\mathrm{eff}} + \chi_\parallel k_\parallel^2)](t - t'). \tag{9}$$

As fluctuation response must damp as time increases, $\gamma_k^{nl} - \gamma_k^{\mathrm{eff}} + \chi_\parallel k_\parallel^2 > 0$. In the first term of Eq. (6), $\partial \tilde{T}^*_{k''}/\partial r$ can be approximated as $-ik_r'' \tilde{T}^*_{k''}$ on fast variation length scales, k_r^{-1}, because nonlinear interactions are restricted within a range of several mode widths.

Under the Markovian approximation,[11] the eddy-damping rate is larger than the rate of spectrum evolution. Therefore, the two-time correlation function can be expressed in the form of

$$\langle \tilde{T}_{k''}(t) \tilde{T}^*_{k''}(t') \rangle = \langle \tilde{T}^2(t) \rangle_{k''} \exp[-(\gamma_{k''}^{nl} - \gamma_{k''}^{\mathrm{eff}} + \chi_\parallel k_\parallel''^2)](t - t'). \tag{10}$$

Then the divergence of the radial flux of fluctuation intensity is

$$\frac{\partial}{\partial r}\langle \tilde{V}_r \tilde{T}^2 \rangle = \sum_k \sum_{k=k'+k''} \Theta_{k,k',k''} \left(\frac{k'_\theta}{k'_\parallel} \right)^2 \frac{v_0^2}{\langle T \rangle^2} I_{k'}(-k_r''^2 I_{k''} + k_r^2 I_k) - \frac{\partial}{\partial r} \left(\sum_k \sum_{k=k'+k''} \Theta_{k,k',k''} \frac{k'_\theta k''_\theta}{k'_\parallel k''_\parallel} \frac{v_0^2}{\langle T \rangle^2} I_{k''} \frac{\partial I_k}{\partial r} \right), \tag{11}$$

where $v_0 = c_t E_0/B_z$ is determined by the mean electric field and toroidal magnetic field, and $I_k = \langle \tilde{T}^2(t) \rangle_k$ is the thermal fluctuation intensity of mode k; the spectrum integral thermal fluctuation intensity is $I = \langle \tilde{T}^2(t) \rangle = \Sigma_k I_k$. The triad mode interaction (or nonlinear mode decorrelation) time is[10,13,23]

$$\begin{aligned} \Theta_{k,k',k''} &= |\gamma_k^{nl} - \gamma_k^{\mathrm{eff}} + \chi_\parallel k_\parallel^2 \\ &\quad + \gamma_{k'}^{nl} - \gamma_{k'}^{\mathrm{eff}} + \chi_\parallel k_\parallel'^2 + \gamma_{k''}^{nl} - \gamma_{k''}^{\mathrm{eff}} + \chi_\parallel k_\parallel^2|^{-1} \\ &\sim |\gamma_k^{nl} + \gamma_{k'}^{nl} + \gamma_{k''}^{nl}|^{-1} \\ &\sim |\chi_\parallel k_\parallel^2 + \chi_\parallel k_\parallel'^2 + \chi_\parallel k_\parallel''^2|^{-1}, \end{aligned} \tag{12}$$

because the relations of $\gamma_k^{\text{eff}} \sim \chi_\parallel k_\parallel^2$ and $\gamma_k^{nl} \sim D_k^{nl}/(\Delta_k^c)^2 \sim \chi_\parallel k_\parallel^2$ are satisfied at the saturated state.

Finally, we obtain the evolution of the thermal fluctuation intensity,

$$\frac{\partial I}{\partial t} - \frac{\partial}{\partial r}\left(\sum_k D_k^{nl}(I)\frac{\partial I_k}{\partial r}\right) = 2\sum_k (\gamma_k^{\text{eff}} - \chi_\parallel k_\parallel^2) I_k + S_{\text{noise}} - S_{\text{diss}}, \tag{13}$$

where

$$D_k^{nl}(I) = \sum_{k=k'+k''} \Theta_{k,k',k''} \frac{k'_\theta}{k'_\parallel}\frac{k''_\theta}{k''_\parallel}\frac{v_0^2}{\langle T\rangle^2} I_{k'}$$

is the nonlinear intensity scattering diffusivity,

$$S_{\text{noise}} = \sum_k \sum_{k=k'+k''} \Theta_{k,k',k''} k_r''^2 \left(\frac{k'_\theta}{k'_\parallel}\right)^2 \frac{v_0^2}{\langle T\rangle^2} I_{k'} I_{k''}$$

is the nonlinear noise, and

$$S_{\text{diss}} = \sum_k \sum_{k=k'+k''} \Theta_{k,k',k''} k_r^2 \left(\frac{k'_\theta}{k'_\parallel}\right)^2 \frac{v_0^2}{\langle T\rangle^2} I_{k'} I_k$$

is the nonlinear dissipation. The nonlinear diffusion term comes from the third term of Eq. (11), while the nonlinear dissipation and noise are from the second and first terms, respectively. This is different from the K-ε model which has both a nonlinear diffusion term and a nonlinear dissipation term, but not a nonlinear noise term. During the triad mode interactions, two beat modes satisfying the resonance condition of $k = k' + k''$ beat together to excite another new mode (i.e., the test mode), while at the same time the excited mode is also dissipated or damped by other modes via nonlinear scrambling. The energy flows from the background modes to the test mode during the excitation process and returns back during the dissipation process. In general, the energy is neither gained nor lost by the test mode, but rather flows through it. The nonlinear diffusion acts as a local energy flux in radius. Thus, the source S_{noise} and the sink S_{diss} conserve the energy via the triad mode energy transfer process in the plasma. The nonlinear diffusion term vanishes at boundaries upon integral to end points.

Contrasting the results with the two claims above, we find that they are consistent. Considering the relation between k_r (or k_r'') and the radial derivative $\partial/\partial r$, we can easily see that all the nonlinear terms (such as noise, dissipation, and diffusion) satisfy the constraint of having the form of $\nabla \cdot J$, the same as the first prediction. Since $I_{k'}(x') = I_k(x + \Delta_1)$ and $I_{k''}(x'') = I_k(x + \Delta_2)$ under the assumption of different modes having the same radial Gaussian structure, the second claim is also fulfilled.

III. DYNAMICS AT SATURATION

The amplitude dependent radial nonlinear diffusion scatters fluctuation energy to nearby regions to be dissipated there by parallel thermal conduction. The system then reaches the saturation state when the radially scattered intensity flux balances the energy dissipated by parallel thermal conduction. Using the nonlinear evolution equation for thermal fluctuation intensity derived above, we can then calculate the scale of nonlinear diffusion for the saturated state in this section. The residual, i.e., nonzero difference of nonlinear noise and dissipation effects, is calculated on the scale of the test mode k, and its influence on intensity front speed is also discussed.

A. Energy conservation

In this study, all free energy comes from the background mean temperature profile, and the total energy is conserved in a self-consistent way. By integrating Eq. (13) over the system size, we obtain

$$2\frac{\partial \varepsilon_T}{\partial t} - \int_0^a dr \frac{\partial}{\partial r}\left(\sum_k D_k^{nl}(I)\frac{\partial I_k}{\partial r}\right) = \int_0^a dr (S_{\text{noise}} - S_{\text{diss}}), \tag{14}$$

with the effective growth term balancing the thermal conduction term at saturation, i.e.,

$$\int_0^a dr \sum_k (\gamma_k^{\text{eff}} - \chi_\parallel k_\parallel^2) I_k = 0. \tag{15}$$

The total energy of thermal fluctuation is defined as $\varepsilon_T = \int_0^a I/2 dr$. The nonlinear noise term cancels the nonlinear dissipation term (shown in Sec. IV A), i.e.,

$$\Delta S = S_{\text{noise}} - S_{\text{diss}} = \sum_k D_k^{nl}(I)(k_r''^2 I_{k''} - k_r^2 I_k) = 0,$$

where $D_k^{nl}(I) = \Sigma_{k=k'+k''}\Theta_{k,k',k''}(k'_\theta/k'_\parallel)^2(v_0^2/\langle T\rangle^2) I_{k'}$, $k_r''^2 = (x + \Delta_2)^2/w^4$, $k_r^2 = x^2/w^4$, and $I_{k''}(x'') = I_k(x + \Delta_2)$, and the diffusion term vanishes at free boundaries (i.e., $\partial I/\partial r = 0$ at boundaries), i.e.,

$$\int_0^a dr \frac{\partial}{\partial r}\left(\sum_k D_k^{nl}(I)\frac{\partial I_k}{\partial r}\right) = \left[\sum_k D_k^{nl}(I)\frac{\partial I_k}{\partial r}\right]_0^a = 0,$$

so the total fluctuation energy is conserved at saturation, as it must be

$$\frac{\partial \varepsilon_T}{\partial t} = 0. \tag{16}$$

B. Correlation length scale

In RGDT, the correlation length Δ_c is determined by the local balance between source and sink. Δ_c tells how far away free energy is scattered from the point where it is topped. Once the correlation length is large enough to exceed the distance between the rational surfaces of two adjacent modes, the radial propagation of fluctuation intensity involves transferring energy from mode to mode. To calculate the correlation length, we can use the saturation criterion of Eq. (15), which can be rewritten as

$$\int_0^a dr \sum_k c_t \frac{k_\theta}{k_\parallel}\frac{E_0}{B_z L_T} I_k = \int_0^a dr \sum_k \chi_\parallel k_\parallel^2 I_k. \tag{17}$$

The ratio of poloidal mode number to toroidal mode number is $k_\theta/k_\parallel = L_s/x$, where $x = r - r_k$ is the displacement away from the rational surface of test mode k, and $L_s = R_0 q^2/rq'$ is the

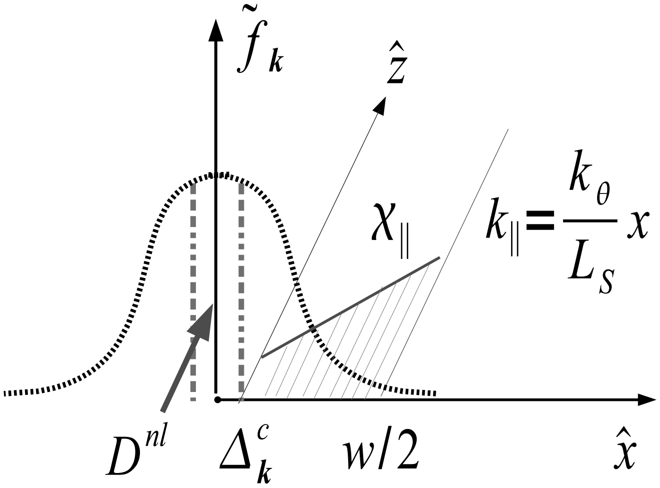

FIG. 5. Energy transfer and dissipation processes.

magnetic shear length. Hence, saturation occurs for the correlation length

$$\Delta_k^c \sim \left(c_t \frac{L_s E_0}{L_T B_z} \right)^{1/3} (\chi_\parallel k_\parallel'^2)^{-1/3}. \tag{18}$$

Here, $k_\parallel' = dk_\parallel / dx = k_\theta / L_s$ is the radial derivative of the parallel mode number. The correlation length can be viewed as the critical radial length for the balance between source, i.e., the linear growth, and sink, i.e., thermal conduction. Δ_k^c depends on the poloidal mode number. Thus, Δ_k^c is a typical nonlinear radial length scale, different from that length scale of the thermal conduction layer in the linear regime.

C. Scale of nonlinear diffusion

Since the propagation of intensity flux is a key element in the dynamics of turbulence spreading and nonlinear diffusive scattering is an important part of the flux, the nonlinear diffusion scale is important in calculating the turbulence spreading speed. During the turbulence spreading, free energy is scattered from the rational surface a certain distance by nonlinear diffusion before being dissipated by radially varying parallel thermal conduction (Fig. 5). Another obvious balance condition in this process is that nonlinear diffusion D_k^{nl} balances the thermal conduction $\chi_\parallel k_\parallel^2$. It determines the radial structure of thermal fluctuation intensity and gives the nonlinear diffusion scale as

$$D_k^{nl} \simeq \left(c_t \frac{L_s E_0}{L_T B_z} \right)^{4/3} (\chi_\parallel k_\parallel'^2)^{-1/3}. \tag{19}$$

As a result of Eq. (13), the nonlinear diffusion is also mode number dependent,

$$D_k^{nl} = \sum_{k=k'+k''} \Theta_{k,k',k''} \frac{k_\theta'}{k_\parallel'} \frac{k_\theta''}{k_\parallel''} \frac{v_0^2}{\langle T \rangle^2} I_{k'}.$$

Transforming the summation into integrals,[37]

$$\sum_{k'} \to \sum_{m'} \sum_{n'} \to \int dm' \int dn',$$

and noting $q = m'/n'$, we get $dn' = (|m'| q'/q^2) dr_{m',n'}$ for the poloidal and toroidal mode numbers (m', n'), where $q' = dq/dr$. Here, we assume $q' > 0$ throughout the integration range of $r_{m',n'}$ from $r-w$ to $r+w$ since nonlinear mode coupling is restricted within the mode width of w (i.e., $\Delta_k^c \le w$ and modes decay fast once $|x| > w$). Hence,

$$\sum_{k'} \to \frac{q'}{q^2} \int |m'| dm' \int_{-w}^{+w} dx'. \tag{20}$$

For simplicity, we make a further approximation of decorrelation time $\Theta_{k,k',k''} \sim 1/\chi_\parallel k_\parallel^2$. The mode k' has a Gaussian radial structure, $I_{k'}(x') = I(r) \exp(-x'^2/2w^2)$, with a slow envelope variation $I(r)$ and a fast variation of $\tilde{f}_{k'}(x') \exp(-x'^2/2w^2)$, where r for the slow length scale (L_T) and x' for the fast length scale (Δ_k^c). This suggests that the fluctuations exponentially decay once $|x'| > w$. The summation of the exponentially dissipating parts is normalized to unit 1 as

$$\sum_{k'} \tilde{f}_{k'}(x') = C_f \frac{q'}{q^2} \int |m'| dm' \int_{-w}^{+w} \exp(-x'^2/2w^2) dx' = 1,$$

where C_f is the normalization coefficient for the fast variation part of the fluctuation intensity. D_k^{nl} is simplified to

$$D_k^{nl} \simeq \left(c_t \frac{L_s E_0}{\Delta_k^c B_z} \right)^2 (\chi_\parallel k_\parallel^2)^{-1} \frac{I}{\langle T \rangle^2}. \tag{21}$$

Comparing Eq. (21) with Eq. (19), we find that the correlation length of test mode k,

$$(\Delta_k^c)^2 \sim \frac{I}{\langle T \rangle^2} L_T^2, \tag{22}$$

which is dependent on the amplitude of intensity.

The nonlinear diffusion coefficient for the mode k has thus been calculated for the saturated state. For a typical mode, we approximate k_θ^2 with its mean square value, i.e.,

$$D^{nl} \simeq \left(c_t \frac{L_s E_0}{L_T B_z} \right)^{4/3} (\chi_\parallel \bar{k}_\parallel'^2)^{-1/3}, \tag{23}$$

where $\bar{k}_\parallel' = (k_\theta)_{\rm rms} / L_s$ is the average of $k_\parallel'$ obtained by calculating the rms value. Similarly, a typical correlation length is approximated by

$$\Delta_c \simeq \left(c_t \frac{L_s E_0}{L_T B_z} \right)^{1/3} (\chi_\parallel \bar{k}_\parallel'^2)^{-1/3}. \tag{24}$$

IV. FRONT SPEED OF TURBULENCE SPREADING

The background mean temperature profile is assumed to be varying slowly in driving turbulence spreading. The question is then how fast the fluctuation intensity front propagates in a given mean temperature profile. Theoretically, a constant front propagating speed, $v_f = 2\sqrt{\gamma D}$, is given by the classic reaction-diffusion equation: Fisher–Kolmogoroff–Petrovsky–Piscounoff (Fisher–KPP) equation.[33–35] We refer to this speed as the Fisher front speed. Our thermal fluctuation intensity evolution equation derived above is also a reaction-diffusion equation, although the diffusion coefficient is nonlinear and depends on the intensity amplitude. The formula of Fisher front speed then can still be applied and is relevant to explain the ballistic propagation in the fast transient experiments, given certain caveats. In this section, we are going to calculate the residual, i.e., nonzero difference of nonlinear noise and dissipation terms, on the scale of the test mode k and discuss the effect of the residual on the front speed.

A. The residual, i.e., nonzero difference of NL noise and NL dissipation terms

Although the spatially integrated noise term cancels the dissipation term, they do not cancel each other locally. This does not conflict with the energy conservation law since conservation is a spatially integrated result, not a local one. For a test mode k, there is thus a modest residual, i.e., nonzero difference of nonlinear noise and dissipation effects, on the scale of the test mode k. This residual influences only the local dynamics of turbulence spreading. Since the magnitude residual is modest, its effects on the front speed is also modest.

First, the total nonlinear residual is calculated by

$$\Delta S = \sum_k \Delta S_k \approx \sum_k D_k^{nl}(k_r''^2 I_{k''} - k_r^2 I_k), \tag{25}$$

where ΔS_k is the residual of the test mode k. Even though the distances between the beat modes and the test mode vary for different k''s and k'''s, we set them to be the same as Δ_k^c, for simplicity. Thus, the thermal fluctuation intensity of the mode k'' can be Taylor expanded in a series of powers of Δ_k^c:

$$\begin{aligned} I_{k''}(x'') &= I(r)\exp\left[-\frac{(x+\Delta_k^c)^2}{2w^2}\right] \\ &= I_k(x)\left[1 - \frac{\Delta_k^c}{w^2}x - \frac{1}{2}\left(\frac{\Delta_k^c}{w}\right)^2\left(1-\frac{x^2}{w^2}\right) + \text{h.o.}\right]. \end{aligned}$$

Here, h.o. represents higher order terms of Δ_k^c which can be ignored. The odd terms in x also vanish upon integration over x, i.e., Σ_k, since $\exp[-x^2/2w^2]$ is an even function. The fast scale mean square derivatives are then $k_r''^2=(x+\Delta_k^c)^2/w^4$ and $k_r^2=x^2/w^4$, respectively. Thus, the residual of mode k is

$$\Delta S_k = D_k^{nl} I_k(x)\left(1 - \frac{5}{2}\frac{x^2}{w^2} + \frac{1}{2}\frac{x^4}{w^4}\right)\left(\frac{\Delta_k^c}{w^2}\right)^2. \tag{26}$$

The odd terms have not been included above because they vanish upon integration over x. By keeping only the first term, and ignoring the other two higher order terms in Eq. (26), the residual of the test mode k at $|x|=\Delta_k^c$ is approximated as

$$\Delta S_k \simeq D_k^{nl} I \exp\left[-\frac{1}{2}\left(\frac{\Delta_k^c}{w}\right)^2\right]\left(\frac{\Delta_k^c}{w^2}\right)^2. \tag{27}$$

Since the correlation length is amplitude dependent, i.e., $\Delta_k^c \sim L_T I^{1/2}/\langle T\rangle$, and $D_k^{nl} \sim \chi_\| k_\|^2 (\Delta_k^c)^2 \sim \gamma_k^{\text{eff}}(\Delta_k^c)^2 \sim c_t L_s E_0 I^{1/2}/B_z\langle T\rangle$ at saturation, the residual is simplified to $\Delta S_k \sim \alpha I^{5/2}$, where $\alpha = c_t L_s L_T^2 E_0/B_z\langle T\rangle^3 w^4$. However, once we sum over all the residuals of test modes,

$$\begin{aligned} \Delta S \approx D^{nl} I\left(\frac{\Delta^c}{w^2}\right)^2 C_f \frac{q'}{q^2}\int |m| dm \int dx\left(1 - \frac{5}{2}\frac{x^2}{w^2} + \frac{1}{2}\frac{x^4}{w^4}\right) \\ \times\exp\left(-\frac{x^2}{2w^2}\right) = 0, \end{aligned}$$

we can see there is no net residual, only a local residual. This shows that the nonlinear noise and the dissipation effects indeed cancel each other upon the summation over all modes, as required by energy conservation. However, localized small residuals survive. In our simplified model, the localized residuals bring a correction to the Fisher front speed for turbulence spreading. In particular, these residuals may lead to modest variations of the front speed at low q rational surfaces, which are discussed below.

B. Fisher front speed without the residual

Before studying the influence of the residual, we first calculate the Fisher front speed of turbulence spreading without the residual. The intensity equation without the noise and dissipation terms is simply

$$\frac{\partial I}{\partial t} - \frac{\partial}{\partial r}\left(D^{nl}\frac{\partial I}{\partial r}\right) = 2\sum_k (\gamma_k^{\text{eff}} - \chi_\| k_\|^2) I_k, \tag{28}$$

where the effective growth can be approximated, by using the correlation length Δ_k^c of mode k at saturation, i.e.,

$$\gamma_k^{\text{eff}} = c_t \frac{L_s E_0}{L_T B_z}\frac{1}{\Delta_k^c}.$$

Using the method of transforming summation into integration as in Sec. III C, both the effective growth and the thermal conduction terms can be calculated as follows:

$$\begin{aligned} \sum_k \gamma_k^{\text{eff}} I_k = \left(c_t \frac{L_s E_0}{L_T B_z} I\right) C_f \frac{q'}{q^2}\int |m| dm \int_{-w}^{+w} \exp\left(-\frac{x^2}{2w^2}\right) \Big/ \\ \Delta_k^c dx \approx c_t \frac{L_s E_0}{L_T B_z} I/\Delta^c, \end{aligned} \tag{29}$$

$$\begin{aligned} \sum_k \chi_\| k_\|^2 I_k &= C_f \frac{q'}{q^2}\int |m| dm \int_{-w}^{+w} dx \chi_\|\left(\frac{m}{rL_s}\right)^2 (\Delta_k^c)^2 I \\ &\quad \times\exp\left(-\frac{x^2}{2w^2}\right) \\ &\approx \chi_\| \bar{k}_\|'^2 (\Delta^c)^2 I. \end{aligned} \tag{30}$$

Here, Δ^c is the value of Δ_k^c at $k_\|' = \bar{k}_\|'$, and $\gamma^{\text{eff}} = c_t L_s E_0/L_T B_z \Delta^c$ as the effective growth rate, independent of k.

The local fluctuation energy is scattered in two steps. First, the effective growth logistically limits local saturation and sets an amplitude dependent correlation length, $\Delta_c \sim L_T I^{1/2}/\langle T\rangle$, to balance source and sink. Second, this correlation length defines an effective nonlinear scattering length for fluctuation intensity, $D^{nl} \sim \chi_{\parallel} k_{\parallel}^2 (\Delta_c)^2 \sim c_t L_s E_0 I^{1/2} / B_z \langle T \rangle$. The spatial coupling effect induced by such nonlinear diffusion then combines with the local growth to produce a Fisher–KPP front velocity of $v_f \approx 2\sqrt{\gamma^{\text{eff}} D^{nl}}$. In our case, the Fisher front speed at saturation is determined by the nonlinear diffusion coefficient and the effective growth rate and is

$$v_f \approx 2\sqrt{\gamma^{\text{eff}} D^{nl}} \approx 2(c_t L_s E_0 / L_T B_z). \tag{31}$$

Of course, the front propagation is ballistic, i.e., $d(t) \sim \bar{v}t$, with a finite constant speed $v_f \sim c_t L_s E_0 / L_T B_z$, and intrinsically nondiffusive. Note that in a reaction-diffusion equation, diffusion and growth (i.e., reaction) combine to yield a nondiffusive front speed. This nontrivial envelope dynamics, spreading at the velocity v_f, occurs on length scales greater than the mode correlation length, but smaller than the mean profile gradient length, i.e., the ordering $\Delta_c < L_f < L_T$ is required for consistency. Front propagation occurs on time scales longer than the fluctuation cascade time, but shorter than fluctuation transport time scales, i.e., $\tau_c^{-1} > v_f / L_f > D / L_T^2$. Thus, intensity front propagation is a prime example of the mesoscale dynamics of turbulence spreading.

More generally, the results of this section suggest that turbulence intensity front can be defined if the scale ordering $\Delta_c < L_f < L_T$, i.e., fluctuation correlation length < front leading edge scale < characteristic profile scale length. In that case, the front will have a characteristic velocity $v \sim (D_T / \tau_c)^{1/2}$, where D_T is the turbulent diffusivity and τ_c is the turbulence correlation time. In this picture, local balance of growth and nonlinear coupling to dissipation define the local saturation level, and the front propagates by turbulent diffusive scattering. Hence, $v_f \sim (D_T / \tau_c)^{1/2}$ emerges as a useful candidate front speed in the quasisaturated state.

C. Fisher front speed with the residual

We now study the effect of the residual on the front speed. The spectral equation of thermal intensity with the residual of test mode k can be rewritten as

$$\frac{\partial I_k}{\partial t} - \frac{\partial}{\partial r}\left(D_k^{nl} \frac{\partial I_k}{\partial r}\right) = 2(\gamma_k^{\text{eff}} - \chi_{\parallel} k_{\parallel}^2) I_k + \alpha_k I_k, \tag{32}$$

where

$$\alpha_k = c_t \frac{L_s E_0}{L_T B_z} \frac{(\Delta_k^c)^3}{w^4}$$

is the coefficient of the residual of mode k at saturation. The dynamics of saturation with the residual are somewhat different from those discussed in the previous section, because there is now an extra effective source in addition to the growth term, which comes from incoherent mode coupling. Then the nonlinear diffusion and the correlation length are readjusted to a new balance between the sources and the sink, and finally reach a new saturated state. Similarly, the correlation length can be recalculated from

TABLE II. Front speeds of turbulence intensity with and without the residual.

Residual	Correlation length	Front speed
Without (macro)	$\left(c_t \frac{L_s E_0}{L_T B_z}\right)^{1/3} (\chi_{\parallel} \bar{k}_{\parallel}'^2)^{-1/3}$	$v_f = c_t \frac{L_s E_0}{L_T B_z}$
With (micro)	$\Delta_k^c \left[1 + \frac{1}{3}\left(\frac{\Delta_k^c}{w}\right)^4\right]$	$v_f \left[1 + \frac{1}{2}\left(\frac{\Delta_k^c}{w}\right)^4\right]$

$$\chi_{\parallel} k_{\parallel}'^2 \Delta_k^2 = \left(c_t \frac{L_s E_0}{L_T B_z}\right) \Big/ \Delta_k + \alpha_k, \tag{33}$$

which denotes the local total source balance with the local sink at the rational surface of the test mode k. Equation (33) has only one real root, approximately,

$$\Delta_k \approx \Delta_k^c \left(1 + \frac{1}{3}(\Delta_k^c / w)^4\right) = \Delta_k^s.$$

The readjusted correlation length, Δ_k^s, is slightly larger than that without the residual. It means that the saturated layer width of the test mode k is slightly expanded when the residual drive is included. Then the nonlinear diffusion coefficient also increases, $D_k^{nl} \approx \chi_{\parallel} k_{\parallel}'^2 (\Delta_k^s)^4$. The free energy is transported sequentially by those expanded saturated layers via a nonlinear mode coupling process. Now the Fisher–KPP-like front speed is

$$v_{f,k} \approx 2\sqrt{\gamma_k^{\text{eff}} D_k^{nl}}.$$

Noticing $\gamma_k^{\text{eff}} = c_t L_s E_0 / L_T B_z \Delta_k^s$ at saturation, we then get the front speed

$$v_{f,k} \approx 2\left(c_t \frac{L_s E_0}{L_T B_z}\right)\left[1 + \frac{1}{2}\left(\frac{\Delta_k^c}{w}\right)^4\right]. \tag{34}$$

This result is slightly faster than the overall front speed v_f without the noise residual. However, the basic scaling of the overall front speed is not significantly affected by small local residuals of different modes, because these residuals cancel upon summation over all modes. Therefore, the residual of mode k gives only a modest correction to the average front speed

$$\delta v_{f,k} \sim (\Delta_k^c / w)^4 (c_t E_0 L_s / B_z L_T).$$

This correction can be ignored for the test mode with $\Delta_k^c < w$. The comparison for the fronts speed with and without the residual is listed in Table II.

V. CONCLUSION

In this paper, we have studied the dynamics of turbulence spreading motivated by the problems of fast transient transport and pulse propagation. A simple mean field model equation of fluctuation intensity, including local nonlinear growth, nonlinear dissipation and noise, and decay to small scales via triad mode coupling, has been derived. The dynamics at saturation were analyzed, and the front speeds of turbulence spreading, both with and without the noise residual of the test mode k, have been discussed. This paper both presents new results and places earlier phenomenological models of turbulence spreading on a more systematic basis.

The principal results of this paper are as follows:

(1) The intensity evolution equation, including nonlinear noise, is derived, including triad mode coupling processes. The mean field intensity equation is shown to have the generic form

$$\frac{\partial I}{\partial t} - \frac{\partial}{\partial r}\left(\sum_k D_k^{nl}(I)\frac{\partial I_k}{\partial r}\right) = 2\sum_k (\gamma_k^{\mathrm{eff}} - \chi_\parallel k_\parallel^2) I_k + S_{\mathrm{noise}} - S_{\mathrm{diss}}.$$

Here, γ_k^{eff} is the effective local growth rate, $\chi_\parallel k_\parallel^2$ is the local dissipation rate, and S_{noise} and S_{diss} are the incoherent and coherent parts of triad mode coupling, respectively, so that S_{noise} corresponds to emission and S_{diss} corresponds to damping. $D_k^{nl}(I)$ corresponds to turbulent scattering on the scale of the fluctuation intensity *envelope*. Note that this model tacitly assumes three radial scales such as Δ_k^c, L_f, and L_T (namely, the fluctuation correlation length, the front scale length—this sets the envelope scale—and the gradient scale length), with the ordering $\Delta_k^c < L_f < L_T$. Triad mode interactions occur on the scale Δ_k^c. Integrated spatially, the nonlinear noise self-consistently cancels the dissipation to conserve total—i.e., spatially integrated—energy. However, *local* deviations from energy balance are possible and can be especially strong near resonant surfaces. Both the emission and the dissipation of the fluctuation are taken into account. The nonlinear noise was neglected in previous theoretical models of turbulence spreading.

(2) The local nonlinear saturation is calculated and is consistent with previous results for RGDT. The amplitude dependent radial nonlinear diffusion scatters fluctuation energy, which is ultimately dissipated by parallel thermal conduction. The fluctuation energy is scattered in two steps. First, the *nonlinear* effective growth logistically limits local saturation at an amplitude dependent correlation length, $\Delta_c \sim L_T I^{1/2}/\langle T\rangle$, so as to balance source and sink. Second, this correlation length defines an effective nonlinear scattering diffusivity for the fluctuation intensity $D^{nl} \sim \chi_\parallel k_\parallel^2 (\Delta_c)^2 \sim c_t L_s E_0 I^{1/2}/B_z\langle T\rangle$, so as to transfer free energy from source to sink. The correlation length sets a characteristic length scale relating the source (i.e., the growth and the nonlinear noise) to the sink (i.e., the dissipation). Nonlinear diffusion then acts as an energy transfer process, which delivers fluctuation energy to stable or unexcited regions. This, in turn, drives turbulence spreading.

(3) There is a residual, i.e., nonzero difference of the nonlinear noise and dissipation on the scale of the test mode k, although no *net* residual survives summation of the residuals of all the modes. This test mode residual influences the local dynamics of the fluctuation intensity front propagation. The effects are seen clearly in Table II, where the front speeds with and without the residual are compared with one another. Without the residual, the front speed is a constant at the Fisher front speed, $v_f \sim c_t E_0 L_s/B_z L_T$. If the residual is included, a small correction to the Fisher front speed, $\delta v_{f,k} \sim (c_t E_0 L_s/B_z L_T) \times (\Delta_k^c/w)^4$, is found at low order rational surfaces, depending on the mode number k. The residual can be ignored once the correlation length is less than the mode width, $\Delta_k^c/w < 1$, but should be retained if $\Delta_k^c/w \sim 1$. In that case, the residual can produce an order unity correction to the magnitude of the front speed.

(4) The characteristic scales in this study are mesoscales. All processes, i.e., triad mode interaction, Fisher–KPP front, and turbulence spreading, occur on length scales comparable to or larger than mode correlation length, but smaller than the mean profile gradient length, i.e., $\Delta_c < L_f < L_T$. The time scales are longer than fluctuation cascade time, but shorter than the global transport time scales, i.e., $\tau_c^{-1} > v_f/L_f > D/L_T^2$. Note that a two scale analysis of fluctuation dynamics is required.

(5) All nonlinear terms of triad mode interactions are written in the conservative form of the divergence of a fluctuation intensity flux, i.e., $\nabla\cdot J$, since triad couplings originate from the intensity flux contribution to the fluctuation intensity equation, i.e., $\nabla\cdot\langle \tilde{V}\tilde{T}^2\rangle$. For free boundary conditions (i.e., $\tilde{V}_k=0$ on boundaries), all flux terms vanish upon spatial integration. The total energy is conserved, although local deviations from energy balance are possible. Then fluctuation energy is transferred only between different modes of fluctuations.

The model analyzed here is simple but generic. Note that its basic features:

(a) the coexistence of three length scales, Δ_c, L_f and L_T, with the ordering $\Delta_c < L_f < L_T$;

(b) a local mixing or decorrelation rate, also comparable to the local drive (i.e., growth) rate, i.e., $\gamma \sim 1/\tau_c$, for quasistationary turbulence; and

(c) spatial scattering, most conveniently represented by a turbulent diffusivity D_T,

are common to virtually all turbulence models for confined plasma. Thus, all these models should exhibit spatiotemporal turbulence front propagation at a speed corresponding to the Fisher speed $v_f \sim (D_T/\tau_c)^{1/2}$. Note that the Fisher speed is generic to reaction (growth)-diffusion models, and thus gives a generic answer to the question of how one extracts nondiffusive dynamics from a seemingly diffusive model.

Given the generic character of the intensity front propagation phenomenon, it is interesting to discuss the possible speeds and their scalings for fronts in drift wave turbulence. Of course, drift-ITG (Ion Temperature Gradient) turbulence is the most relevant model for describing cold pulse propagation and other fast transients. For drift wave turbulence, generically, $1/\tau_c$ is set by the diamagnetic frequency, so $1/\tau_c \sim c_s/L_\perp$ [i.e., $k\rho_s \sim o(1)$, and $L_\perp$ is a characteristic gradient scale length]. Similarly, $D_T \sim D_B \rho_*^\alpha$, where $D_B = \rho_s c_s$ is the Bohm diffusivity and $\rho_* = \rho_s/L_\perp$. Here, usually $0 < \alpha < 1$, where $\alpha = 0$ corresponds to Bohm scaling, where $\alpha = 1$ corresponds to gyro-Bohm. Thus, the intensity front speed is predicted to scale as $v_f \sim c_s \rho_*^{(1+\alpha)/2}$, so $v_f \sim c_s \rho_*$ for gyro-Bohm scaling and $v_f \sim c_s \rho_*^{1/2}$ for Bohm scaling. For the experimentally observed scaling exponent of $\alpha \sim 0.7$, $v_f \sim c_s \rho_*^{0.8}$. This gives several testable predictions for the propagation of turbulence pulses, namely,

(i) the magnitude of the speed,
(ii) the speed scaling with B_0, which can be studied with a toroidal field scan, and
(iii) the speed scaling with isotope. Note that $v_f \sim (A_i)^{(\alpha-1)/2}$, so v_f is independent of isotope for the case of gyro-Bohm scaling and $v_f \sim A_i^{-1/2}$ for Bohm. This can be studied by comparing fast transients in hydrogen and deuterium plasmas.

Finally, we note that pulse propagation speed scaling can be used to probe the underlying transport dynamics.

The model discussed here is exceedingly simple, so this work should be regarded as only a beginning. Future work will focus on extensions to more realistic turbulence models with more realistic geometric structure—i.e., drift wave turbulence in a torus. A key question is how nonlinear interaction competes with linear coupling of poloidal subharmonics and with zonal shearing. More fundamentally, one should look past quasilocal diffusion to explore front propagation in systems with nonlocal transport, as recently observed in full f, flux driven ITG simulations.[38] In that case, however, simply replacing the local diffusivity of the Fisher type equation with a nonlocal scattering operator seems inconsistent, as the drive will surely also become nonlocal in the presence of avalanching. Thus, a consistent nonlocal formulation of turbulence spreading dynamics remains an elusive challenge.

ACKNOWLEDGMENTS

The authors would like to thank C. J. McDevitt, T. S. Hahm, G. Dif-Pradalier, and Hong-Juan Sun for useful and thought provoking discussions. Z.H.W. also wants to thank China Scholarship Council and NSFC for supporting his study at UCSD. This research was also supported by the U.S. Department of Energy Contract Nos. DE-FG02-04ER54738, DE-FC02-08ER54983, and DE-FC02-08ER54959 and by the Ministry of Education, Science and Technology of Korea via WCI Project No. 2009-001. Z.H.W. and X.G.W. were also supported by NSFC Grant Nos. 40731056, 10778613, 10575018, and 10675029 and National Basic Research Program of China Grant Nos. 2008CB787103 and 2009GB105004.

[1] P. Mantica, D. Van Eester, X. Garbet, F. Imbeaux, L. Laborde, M. Mantsinen, A. Marinoni, D. Mazon, D. Moreau, N. Hawkes, E. Joffrin, V. Kiptily, S. Pinches, A. Salmi, S. Sharapov, A. Thyagaraja, I. Voitsekhovitch, P. de Vries, and K.-D. Zastrow, Phys. Rev. Lett. **96**, 095002 (2006).
[2] K. W. Gentle, R. V. Bravenec, G. Cima, H. Gasquet, G. A. Hallock, P. E. Phillips, D. W. Ross, W. L. Rowan, A. J. Wootton, T. P. Crowley, J. Heard, A. Ouroua, P. M. Schoch, and C. Watts, Phys. Plasmas **2**, 2292 (1995).
[3] H. J. Sun, X. T. Ding, L. H. Yao, B. B. Feng, Z. T. Liu, X. R. Duan, and Q. W. Yang, Plasma Phys. Controlled Fusion **52**, 045003 (2010).
[4] P. Beyer, S. Benkadda, X. Garbet, and P. H. Diamond, Phys. Rev. Lett. **85**, 4892 (2000).
[5] A. Rocco, U. Ebert, and W. van Saarloos, Phys. Rev. E **62**, R13 (2000).
[6] C. Holland, P. H. Diamond, S. Champeaux, E. Kim, Ö. D. Gürcan, M. N. Rosenbluth, G. R. Tynan, N. Crocker, W. Nevins, and J. Candy, Nucl. Fusion **43**, 761 (2003).
[7] Z. Lin and T. S. Hahm, Phys. Plasmas **11**, 1099 (2004).
[8] T. S. Hahm, P. H. Diamond, Z. Lin, K. Itoh, and S.-I. Itoh, Plasma Phys. Controlled Fusion **46**, A323 (2004).
[9] V. Naulin, A. H. Nielsen, and J. Juul Rasmussen, Phys. Plasmas **12**, 122306 (2005).
[10] A. Hasegawa and K. Mima, Phys. Fluids **21**, 87 (1978).
[11] R. H. Kraichnan, J. Fluid Mech. **5**, 497 (1959).
[12] P. H. Diamond, M. N. Rosenbluth, F. L. Hinton, M. Malkov, J. Fleischer, and A. Smolyakov, *Proceedings of the 17th International Conference on Fusion Energy*, Yokohama, Japan (International Atomic Energy Agency, Vienna, 1998), Paper TH3/1.
[13] V. B. Lebedev, P. H. Diamond, V. D. Shapiro, and G. I. Soloviev, Phys. Plasmas **2**, 4420 (1995).
[14] Ö. D. Gürcan, P. H. Diamond, T. S. Hahm, and Z. Lin, Phys. Plasmas **12**, 032303 (2005).
[15] Ö. D. Gürcan, P. H. Diamond, and T. S. Hahm, Phys. Rev. Lett. **97**, 024502 (2006).
[16] P. H. Diamond and T. S. Hahm, Phys. Plasmas **2**, 3640 (1995).
[17] P. H. Diamond, S. Chapeaux, M. Malkov, A. Das, C. Holland, B. Wecht, A. I. Smolyakov, F. L. Hinton, Z. Lin, and T. S. Hahm, Nucl. Fusion **41**, 1067 (2001).
[18] X. Garbet and R. E. Waltz, Phys. Plasmas **5**, 2836 (1998).
[19] Y. Sarazin, X. Garbet, P. Ghendrih, and S. Benkadda, Phys. Plasmas **7**, 1085 (2000).
[20] P. A. Politzer, Phys. Rev. Lett. **84**, 1192 (2000).
[21] P. Bak, C. Tang, and K. Wiesenfeld, Phys. Rev. Lett. **59**, 381 (1987).
[22] X. Garbet and R. E. Waltz, Phys. Plasmas **3**, 1898 (1996).
[23] Ö. D. Gürcan, P. H. Diamond, and T. S. Hahm, Phys. Plasmas **13**, 052306 (2006).
[24] X. Garbet, Y. Sarazin, F. Imbeaux, P. Ghendrih, C. Bourdelle, Ö. D. Gürcan, and P. H. Diamond, Phys. Plasmas **14**, 122305 (2007).
[25] P. H. Diamond, V. B. Lebedev, D. E. Newman, and B. A. Carreras, Phys. Plasmas **2**, 3685 (1995).
[26] P. H. Diamond, V. B. Lebedev, D. E. Newman, B. A. Carreras, T. S. Hahm, W. M. Tang, G. Rewoldt, and K. Avinash, Phys. Rev. Lett. **78**, 1472 (1997).
[27] S. Chandrasekhar, Rev. Mod. Phys. **15**, 1 (1943).
[28] F. Imbeaux, F. Ryter, and X. Garbet, Plasma Phys. Controlled Fusion **43**, 1503 (2001).
[29] Y. Kishimoto, T. Tajima, W. Horton, M. J. LeBrun, and J. Y. Kim, Phys. Plasmas **3**, 1289 (1996).
[30] S.-I. Itoh and K. Itoh, Plasma Phys. Controlled Fusion **43**, 1055 (2001).
[31] L. Garcia, P. H. Diamond, B. A. Carreras, and J. D. Callen, Phys. Fluids **28**, 2147 (1985).
[32] T. S. Hahm, P. H. Diamond, P. W. Terry, L. Garcia, and B. A. Carreras, Phys. Fluids **30**, 1452 (1987).
[33] R. A. Fisher, Annu. Eugen. **7**, 355 (1937).
[34] A. Kolmogoroff, I. Petrovsky, and N. Piscounoff, Clin. Cancer Res. **1**, 1 (1937).
[35] J. D. Murray, *Mathematical Biology* (Springer-Verlag, New York, 1993), p. 274.
[36] P. H. Diamond, S.-I. Itoh, and K. Itoh, *Physical Kinetics of Turbulent Plasmas*, Modern Plasma Physics (Cambridge University Press, New York, 2010), Vol. I, p. 150.
[37] P. H. Diamond and M. N. Rosenbluth, Phys. Fluids **24**, 1641 (1981).
[38] G. Dif-Pradalier, P. H. Daimond, V. Grandgirard, Y. Sarazin, J. Abiteboul, X. Garbet, Ph. Ghendrih, A. Strugarek, S. Ku, and C. S. Chang, Phys. Rev. E **82**, 025401(R) (2010).